



Toward the first light of the Layer Oriented Wavefront Sensor for MAD

C. Arcidiacono¹, M. Lombini², J. Farinato¹, and R. Ragazzoni¹

¹ Istituto Nazionale di Astrofisica – Osservatorio Astronomico di Padova, Vicolo dell'Osservatorio 5, I-35122 Padova

e-mail: carmelo.arcidiacono@oapd.inaf.it Italy

² Istituto Nazionale di Astrofisica – Osservatorio Astrofisico di Arcetri, L. E. Fermi 5, I-50125 Firenze

Abstract. MAD is the ESO demonstrator for the Multiconjugate Adaptive Optics technique in the framework of the European Extremely Large Telescope design. The instrument accommodates two wavefront sensors: a Star Oriented multi Shack–Hartmann and a Layer Oriented multi pyramid. It is installed on the UT3 unit of the Very Large Telescope and it is completed by the CAMCAO scientific Infrared camera, with a $2K \times 2K$ infrared detector movable over the 2arcmin corrected Field of View. In March 2007 the instrument had the first light at the telescope using the star oriented approach. In this paper we report on the test for the Preliminary Acceptance Europe for the Layer Oriented wavefront sensor which was successfully passed giving green light for the forthcoming installation and the Layer Oriented first light expected for September 2007.

Key words. Instrumentation: Adaptive Optics

1. Introduction

The ESO Multi conjugate Adaptive optics Demonstrator Marchetti & al. (2003, 2005) was conceived to demonstrate the MCAO–technique feasibility and to characterize the performance using both Star Oriented (SO) multi Shack–Hartmann (SHWFS) WFSs configuration and the Layer Oriented (LO) multi–pyramid approach (LOWFS) Vernet–Viard & al. (2003); Viard & al. (2005). The two sensors have been integrated on the MAD bench and tested in laboratory in Garching (ESO, Germany) to be finally delivered to Paranal (Chile). The MAD instrument is mounted on a single bench, which now is installed on

Send offprint requests to: C. Arcidiacono

the Nasmyth–B platform of the Very Large Telescope (VLT) UT–3 unit for the commissioning. The MAD–bench is not fixed to the Nasmyth adapter rotator flange, then the pupil rotates with the field: an optical de–rotator at the entrance of the adaptive–system rotates both. The adaptive system is composed by common, to both WFSs, re–imaging optics collimating the F/15 input beam, in order to re–image the telescope pupil on the two bimorph deformable mirrors (XINETICS with 60 actuators each). Both WFSs and DMs look to a region of 2'Field of View (FoV). The larger DM, 100 mm diameter, is conjugated to 8.5 km altitude, while the smaller DM with a 60 mm pupil is conjugated to the re–imaged telescope pupil for ground layer correction. The

IR light is transmitted by the dichroic to the CAMCAO scientific IR camera while the visible light is reflected toward the WFS path. The MAD bench common optics retrieves to the WFS a flat telecentric F/20 input beam. The CAMCAO chip is based on a $2K \times 2K$ Hawaii2 IR detector controlled by a standard IRACE system: it covers a 1 arcmin square area with pixel scale of 0.028 arcsec/pixel, Nyquist sampling in K Band, built by the Universidad de Lisboa. The camera has standard IR band filters (**J** ($1.25 \mu\text{m}$), **H** ($1.65 \mu\text{m}$), **K'** ($2.12 \mu\text{m}$), Br-Gamma and Br-Gamma continuum) mounted on a manually positionable filter wheel. CAMCAO is placed in the F/15 focused beam after the dichroic. Field and pupil cold stops are implemented to significantly reduce the background and the stray-light. The CAMCAO InfraRed camera optics provide diffraction limited images down to **J** ($1.25 \mu\text{m}$) Band. CAMCAO is used to evaluate the wide FoV MCAO correction of MAD thanks to a xy linear stages motions allowing scanning the whole $2'$ FoV by 4 mosaics. Two calibration units are also available. One calibration unit is at the entering F/15 input focus: this calibration unit consists of a set of visible-IR light illuminated fibers supported by a plate. The plate can be moved to scan the whole $2'$ FoV to emulate different NGS positions. A third motion along the optical axis will move along the optical axis. Another calibration unit stays on the WFS path.

The two WFSs cannot be used simultaneously: two different mirrors are mounted on as many linear stages folding the light either to the LO-WFS located above the bench or to the SO WFS which is on the bench. Moreover the two mirrors can be completely removed: in this way the F/20 beam is free to reach a technical camera. This camera has the only purpose to observe the $2'$ field in the optical band and in open loop to find the references actual positions, positioning correctly both Shack Hartmanns and Pyramids.

2. The Layer Oriented WFS

In the LO-WFS for MAD the multi-pyramid approach is exploited: as in single reference

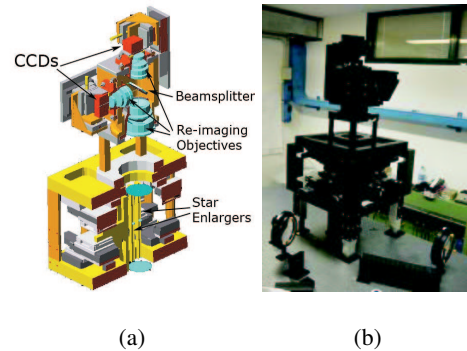


Fig. 1. These figures present the CAD view 1(a) and a real picture 1(b) of the MAD Layer Oriented WFS.

case Ragazzoni (1996); Ragazzoni & Farinato (1999), the light of each reference stars is split into four beams by a pyramid placed on a focal plane and centered on the nominal position of the star. Then a reimaging objective projects on a CCD the pupil images, which super impose according to the conjugation altitude and the stars directions. In the LO-WFS for MAD up to 8 pyramids can be positioned over the $2'$ FoV to catch the light from eight reference guide stars, fig. 1. In the Layer Oriented Ragazzoni (2000); Ragazzoni, Farinato & Marchetti (2000) approach the pupil images are co-added mimicking the super-imposition of the reference stars beams through the atmosphere as they do at the conjugation altitude. In MAD the reference pupils co-addition is optically performed on two different WFSs, which looks simultaneously to four pupil images pupils of all reference stars, thanks to a beam splitter placed on the pupil re-imager optical path splitting the light to two identical objectives. The single pupil image corresponding to the F/20 WFS-input beam is too large to fit the dimensione of wavefront sensing fast read out CCD, even if used with very fast re-imaging optics. In fact the detector size is one crucial parameter to determine the optics characteristics and the final LOWFS optical design was decided to fit this size. The two detectors are EEV39 with 80×80 pixels, with 0.024mm pixel-size corresponding to $1.92 \times 1.92\text{mm}$ sensing re-

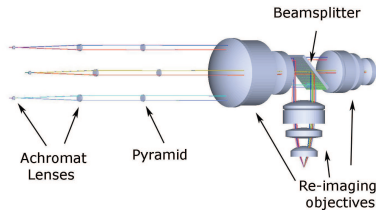


Fig. 2. Optical layout of the LO-WFS. In the real system 8 pyramids are available even if only 3 are shown here. The stars light coming from the left is caught by the system composed by the two achromatic doublets and split by the pyramids. The beams pass through the common path pupil re-imager before to be split to the high and the ground pupil re-imaging objectives. The pupil images are sensed by the two CCDs.

gion. Pupil size shrinking was necessary to fit CCD size: in general this can be achieved by enlarging the focal ratio before the pupil re-imager, but in this way the focal plane corresponding to the 2' field is enlarged of the same factor and the re-imager aperture too. The trick used to still use small re-imaging optics is described in Ragazzoni, & al. (2005) and it consists in enlarging the focal ratio only on the optical path of the reference stars in front of each pyramid. This goal was achieved using a co-moving optical train for each pyramid: two small diameter achromatic doublets have been used to obtain a new F/300 focal plane in correspondence of the pyramids vertex. The second lens diameter fixes the minimum separation between two reference stars: because of their physical dimensions two adjacent pyramids cannot be more close than a distance corresponding to $20''$ (centre-centre) if projected on sky. In this way the pupil has been shrink by a factor 15, and using a very fast F/1.05 reimager, a $\approx 0.388\text{mm}$ pupil size has been obtained. Moreover as small as possible divergence angle for the pyramids have been selected ($\approx 1.2\text{deg}$ opposite pyramid faces tilt angle Arcidiacono (2005)) to accommodate the four pupils on the CCD. Using a fixed 2×2 binning for ground CCD and 4×4 for high one the corresponding 8×8 and 7×7 metapupil spatial sampling have been obtained.

The two CCDs are positioned with great accuracy ($\approx 1\mu\text{m}$) in order to properly conju-

gate to deformable mirrors and corresponding layer altitudes. The CCD are mounted on linear stages movements giving the possibility to re-adjust the position of the conjugated planes. The stages are the same used to move over the 2' FoV the mounting of the optical train (called star enlarger) composed by a pyramid and the 2 achromatic doublets: in fact these 8 mountings are screwed to as many xy couples of linear stages.

3. Tests

The capabilities of the LOWFS coupled to the MAD bench had been extensively tested using the MAPS turbulence simulator Kolb & al. (2005) available at the bench entrance focus. Initially has been identified the best way to record an Interaction Matrix (IM): pushing and pulling actuators forming Hadamard modes a modulation of $\approx 17\lambda_V/D$ on all the pyramids is applied by the Tip Tilt mirror on which the Ground DM is mounted, using enough small core fibers as references (smaller than the modulation amplitude) to en-light efficiently the high altitude DM, once the IM is recorded a control matrix (CM) is computed by matrix inversion, the DMs are flattened by closing loop and average voltages are used as new references for actuators positions and a new IM is then recorded. Moreover we found out that discarding from the correction computation the low signal sub-apertures on the high loop can improve significantly performance. One of the advantages of the LO with respect to the SO is that it is not necessary to record a new IM for each reference stars constellation. Another advantage is in the sensor itself, in fact we checked that the pyramid gain with respect to the SH system in term of limiting magnitude, according to theoretical expectations Ragazzoni & Farinato (1999); Esposito & Riccardi (1996); Verinaud (2004). We studied the single conjugate case (SCAO) to evaluate the achievable performances of the pyramid WFS such as it is configured on the MAD experiment. By using this configuration we analyzed the behavior of the correction with respect to the magnitudes of the reference stars. All magnitude

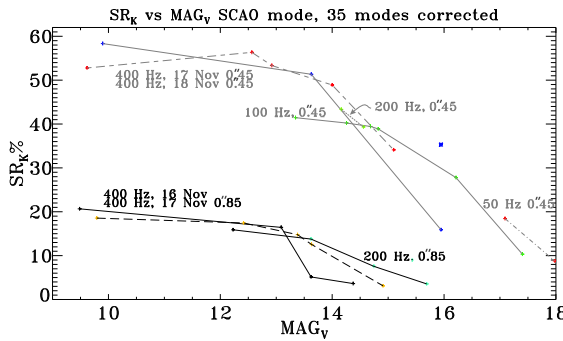


Fig. 3. The SR versus magnitude curve for the SCAO case, in the picture are labeled the conditions used to generate each curves, "0.85" indicates 0.85" seeing atmosphere and "0.45" indicates 0.45" seeing atmosphere, both with speed configuration that gives $\tau_0 = 3\text{ms}$ (0.85"). It is also indicated the read out mode used. Compared to similar plot obtained for the SHWFS on MAD using same atmosphere and fiber source a gain of ≈ 1.5 magnitude has been measured.

for the SCAO Pyramid case has been computed assuming that the collected light interest a single Pyramid Wavefront Sensor. The limiting magnitude computed as the magnitude at which has been obtained half of the bright end SR in SCAO (considering all the used read out modes) have been 16.5 for good seeing (0.45") and 14.5 for bad seeing (0.85"). Compared to similar measurements obtained for the SHWFS Kolb & Marchetti (2007) on MAD using the same atmospheres and fiber source a gain of ≈ 1.5 magnitude has been measured.

4. Conclusions

The full functionality of the sensor for the three possible Adaptive Optics control configurations, SCAO, Ground Layer AO and MCAO, has been demonstrated. The behavior of the LOWFS for different atmospheric seeing conditions has been analyzed, for instance in the case of bad seeing (0.85") we registered in GLAO mode $SR_K \approx 8\%$ with very uniform behavior over the central 1' region and significantly flat over the 2' and a 2.5-3 Ensquared Energy gain with respect to the seeing case in 0.1", in MCAO mode we obtained 24% SR_K with a quite uniform distribution and 33% very

peaked on the centre direction (EE gain w.r.t. seeing ≈ 3.5). The effect of different guide stars configurations has been attacked even if a detailed analysis that goes beyond the test plan is needed to fully understand the relationship between this and the performance over the field: what we can assess is that with a constellation of reference stars concentrated toward a specific direction both GLAO and MCAO corrections act similarly to a SCAO correction in term of distribution of the SR and in term of orientation of the PSF. We identify how to register IM and to compute Control Finally we recorded faint end behavior, in particular we measured the limiting magnitude at half of the bright end performance in various of the allowed modes: for instance a limiting magnitude 16.5 for good seeing and 14.5 for bad seeing has been found.

Acknowledgements. Thanks are due to E. Marchetti, J. Kolb, S. Tordo, C. Soenke, R. Donaldson and S. Oberti for the fundamental support during the laboratory test in Garching and before.

References

- Marchetti, E. & al. 2003, Proc. of SPIE, 4839, 317
- Marchetti, E. & al. 2005, Comptes Rendus de l'Académie des Sciences, Vol. 6, 10, 1118
- Vernet-Viard, E. & al. 2003, Proc. of SPIE, 4839, 344
- Viard, E. & al. 2005, Opt. Eng., 44
- Ragazzoni, R. 1996, Journ. of Mod. Opt., 43, 289
- Ragazzoni R. and Farinato, J. 1999, A&A, 350, L23
- Ragazzoni, R. 2000, *ESO proceedings of the Backaskog workshop on extremely large telescopes*, 57, 175
- Ragazzoni, R., Farinato, J. & Marchetti, E. 2000, Proc. of SPIE, 4007, 1076
- Ragazzoni, R., & al. 2005, PASP, 117, 860
- Arcidiacono, C. 2005, Opt. Com., 252, 239
- Kolb, J., & al. 2004, Proc. of SPIE, 5490, 794
- Esposito, S. & Riccardi, A. 2001, A&A, 369, L9
- Vérinaud, C. 2004, Opt. Com. 233, 27
- Kolb, J. & Marchetti, E., 2007, priv. comm.